Available online at www.sciencedirect.com
ScienceDirect
Journal of Power Sources 177 (2008) 184–193
JOURNAL OF POWER SOURCES
www.elsevier.com/locate/jpowsour

Dynamic behavior of surface film on $LiCoO_2$ thin film electrode

Masaki Matsui [a,b], Kaoru Dokko [b], Kiyoshi Kanamura [b,*]

[a] *Material Engineering Div. 3, Toyota Motor Corporation, 1200 Mishuku, Susono, Shizuoka 410-1193, Japan*
[b] *Department of Applied Chemistry, Graduate School of Urban Environmental Science, Tokyo Metropolitan University, 1-1 Minami-Ohsawa, Hachioji, Tokyo 192-0397, Japan*

Received 23 August 2007; received in revised form 16 October 2007; accepted 23 October 2007
Available online 1 November 2007

Abstract

Electrochemical oxidation behavior of non-aqueous electrolytes on $LiCoO_2$ thin film electrodes were investigated by *in situ* polarization modulation Fourier transform infrared (PM-FTIR) spectroscopy, atomic force microscopy and X-ray photoelectron spectroscopy (XPS). $LiCoO_2$ thin film electrode on gold substrate was prepared by rf-sputtering method. *In situ* PM-FTIR spectra were obtained at various electrode potentials during cyclic voltammetry measurement between 3.5 V vs. Li/Li^+ and 4.2 V vs. Li/Li^+. During anodic polarization, oxidation of non-aqueous electrolyte was observed, and oxidized products remained on the electrode at the potential higher than 3.75 V vs. Li/Li^+ as a surface film. During cathodic polarization, the stripping of the surface film was observed at the potential lower than 3.9 V vs. Li/Li^+. Depth profile of XPS also showed that more organic surface film remained on charged $LiCoO_2$ than that on discharged one. AFM images of charged and discharged electrodes showed that some decomposed products deposited on charged electrode and disappeared from the surface of discharged one. These results indicate that the surface film on $LiCoO_2$ is not so stable.

Keywords: Rechargeable lithium battery; $LiCoO_2$; Non-aqueous electrolyte; Oxidation; Surface film

1. Introduction

Rechargeable lithium battery has high energy density, so that it is attractive as power source for hybrid electric vehicle (HEV). This is accomplished by high cell voltage owing to highly oxidative and reductive active materials used in this battery [1,2]. To realize this high voltage, aprotic non-aqueous solvents have been utilized for electrolyte solutions. In general, propylene carbonate (PC), ethylene carbonate (EC) and diethyl carbonate (DEC), that are popular non-aqueous solvents for rechargeable lithium battery, have wider electrochemical window than operation voltage of this battery [3–5]. However, some research groups have proposed that non-aqueous electrolytes are likely to be oxidized and form surface film on cathode active material like SEI layer on graphite anode [6,7]. Our group also has analyzed electrochemical oxidation of PC or EC and DEC binary solvent on $LiCoO_2$ thin film electrode occurring around 3.8 V vs. Li/Li^+ by *in situ* FTIR measurement and XPS analysis [8–11].

In the case of graphite anode, SEI layer plays an important role for lithium intercalation/de-intercalation. By using EC-based electrolyte solution, SEI layer is usually formed during the first cycle and stably remained on the surface during intercalation/de-intercalation processes continuing in further cycles [12,13]. On the other hand, in the case of PC-based electrolyte, co-intercalation of the solvent molecules occurs, and this phenomenon causes an exfoliation of graphene layers [14]. This exfoliation prevents smooth intercalation/de-intercalation of lithium ion into/from graphite anode. So far, some inorganic and organic compounds have been proposed as electrolyte additives, to improve the stability of SEI layer. Vinylene carbonate (VC) is one of the most popular electrolyte additives for graphite anode. It has been supposed that polymerized VC makes stable SEI layer and improves a cycle performance of batteries [15,16].

Recently, a surface of cathode material has been investigated in order to improve a life performance of rechargeable lithium ion batteries. For instance, a surface of active materials has been covered with non-conducting oxides, such as alumina and zirconia to suppress degradation of cathodes [17,18]. On the other hand, surface analysis on cathode material has been also done to observe a dynamic behavior of cathode material surface [8–11].

* Corresponding author. Tel.: +81 426 77 2828; fax: +81 426 77 2828.
E-mail address: kanamura-kiyoshi@c.metro-u.ac.jp (K. Kanamura).

0378-7753/$ – see front matter © 2007 Elsevier B.V. All rights reserved.
doi:10.1016/j.jpowsour.2007.10.078

In these studies, only anodic polarization behavior of $LiCoO_2$ and $LiMn_2O_4$ has been discussed by using *in situ* FTIR measurement and XPS analysis. In these studies, an electrochemical oxidation of solvents has been detected from 4.0 V vs. Li/Li^+.

In the present study, we also investigated surface film formation process on $LiCoO_2$ thin film electrode by using *in situ* PM-FTIR, XPS and AFM to discuss the stability of the surface film on $LiCoO_2$ during charge and discharge processes. In this study, we focused on organic surface films formed on $LiCoO_2$, so that we selected $LiClO_4$ as the Li-salt to avoid the decomposition of Li-salt. In this work, we employed PM-FTIR in order to realize higher sensitivity for organic compounds formed on $LiCoO_2$ electrode and dynamic behavior of surface film during discharge and charge processes.

2. Experimental

In this study, $LiCoO_2$ thin film electrodes were prepared by rf-sputtering (SPK-301, Tokki). Sputtering conditions were the same with that reported in our previous paper [10,11], and sputtering duration was 90 min. The as-sputtered film was in an amorphous state, so that the thin film was heated at 700 °C for 5 h, in order to improve its crystallinity.

The prepared thin film was analyzed by X-ray diffraction method (RINT-2000, Rigaku) with Cu Kα (40 kV and 40 mA) at a scan rate of $1^\circ\,min^{-1}$ in 2θ range from 10° to 100°. Raman spectroscopy (NRS-1000, Jasco) with 532 nm laser radiation was also utilized to detect hexagonal and cubic phases of $LiCoO_2$.

An oxidation of non-aqueous electrolytes was analyzed by *in situ* PM-FTIR spectroscopy (Nicolet 6700, Thermo Electron). The *in situ* spectroelectrochemical cell for external reflectance method [19] and the optical system for *in situ* PM-FTIR spectroscopy were shown in Fig. 1. *In situ* PM-FTIR spectroscopy was performed using p-polarized and s-polarized IR beam modulated by a photoelastic modulator (PEM-90, Hinds) with Dual-channel Synchronous Sampling Technique Module. A sum-spectrum of p-polarized and s-polarized IR beam was collected by A channel as a background spectrum, and a differential spectrum was collected by B channel as a sample spectrum (Fig. 2). When the IR beam is reflected from electrode, p-polarized beam is strongly absorbed by molecules on the electrode surface, more than s-polarized beam. Therefore, spectrum of the electrolyte solution between window and

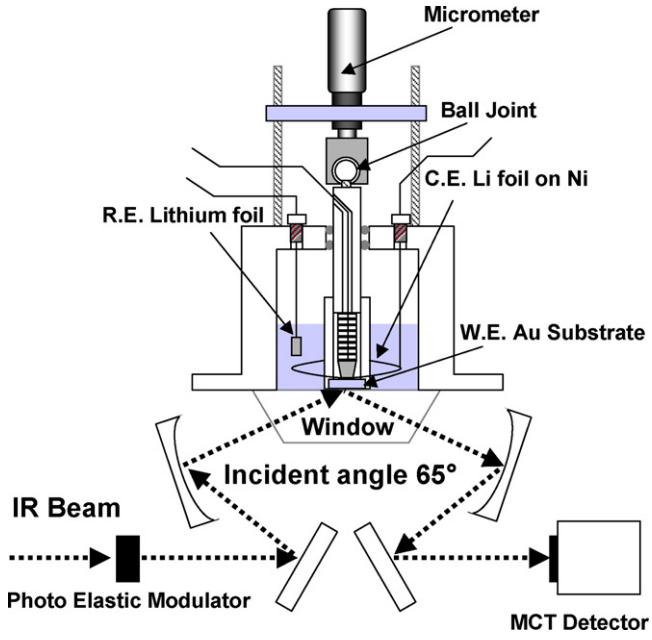

Fig. 1. Schematic illustration of *in situ* PM-FTIR cell and optical system.

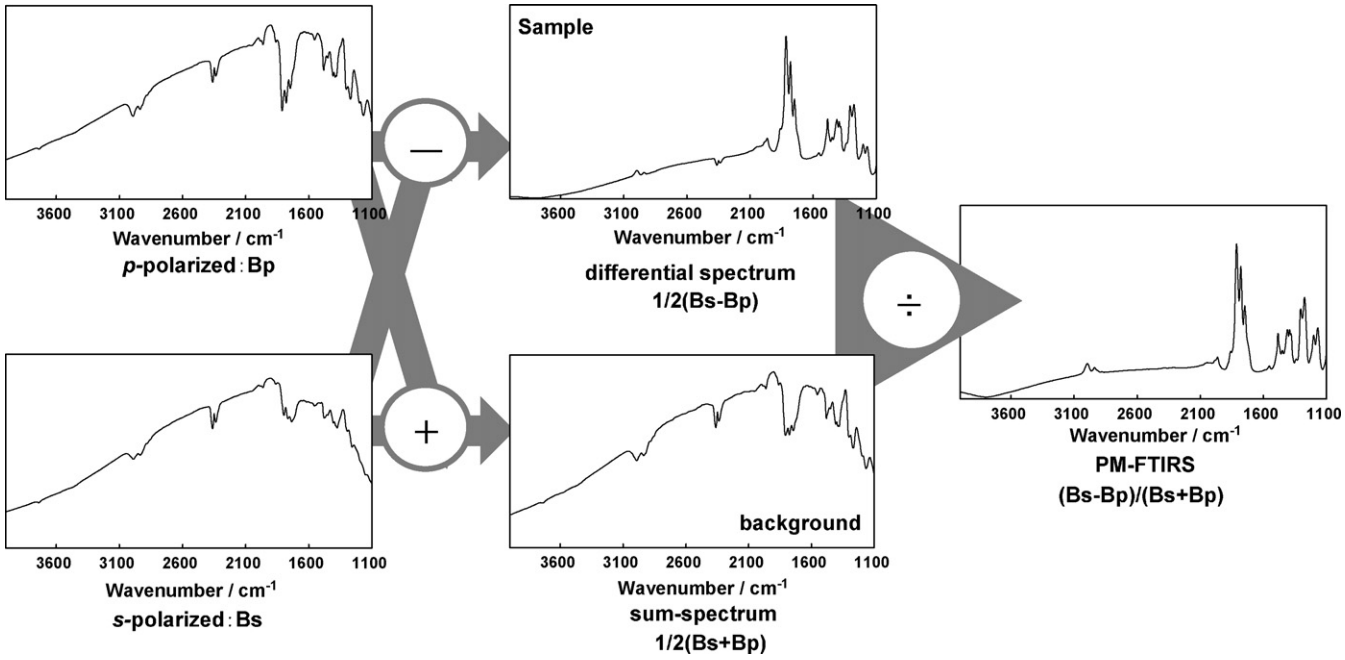

Fig. 2. Spectrum calculation for PM-FTIR.

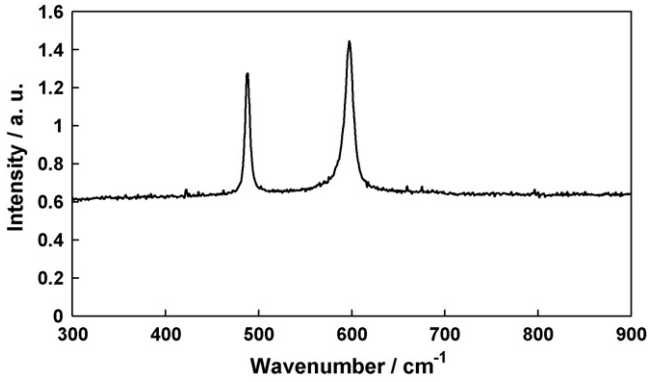

Fig. 3. Raman spectrum of $LiCoO_2$ thin film prepared by using rf-sputtering process.

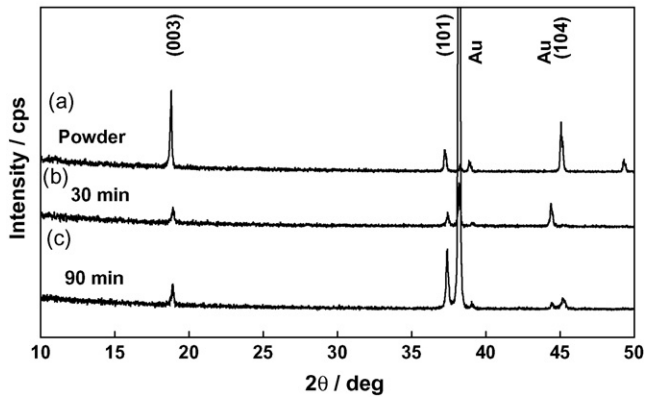

Fig. 4. X-ray diffraction patterns of $LiCoO_2$ powder (a) and thin film electrodes prepared by sputtering process for 30 min (b) and 90 min (c).

electrode is cancelled in this measurement and only the absorption spectrum of the electrode surface is amplified by this technique.

The prepared thin film electrode was used as working electrode and Li metal was used as counter electrode and reference electrode. The electrolyte solutions were 1 mol dm^{-3} $LiClO_4$-PC and 1 M $LiClO_4$-EC: DEC (1:1) (Kishida Chemical Co. Ltd., Japan). CaF_2 was used as IR window. The measured wavenumber region was 1100–2200 cm^{-1}. The accumulation time was 200. *In situ* PM-FTIR spectra were obtained at various electrode potentials during cyclic voltammetry [20]. The potential range was 3.5–4.2 V vs. Li/Li^+ and the sweep rate was 0.1 mV s^{-1}. Interval of *in situ* PM-FTIR measurement was 500 s, so the difference of the electrode potential of each measurement was 50 mV. At each potential, the external reflectance spectrum was measured. Differential spectrum was calculated from two spectra measured at each electrode potential, as an *in situ* PM-FTIR spectrum.

The calculated differential spectra involved upward and downward peaks. The former one corresponds to a disappearance of chemical bond (decrease in amount of substances). The latter one corresponds to a generation of new chemical bonds (increase in amount of new substances).

XPS analysis on the $LiCoO_2$ thin film electrode surface was conducted to observe remaining species on the surface. Two-electrode cell was fabricated with $LiCoO_2$ thin film electrode as cathode and lithium foil as anode. A galvanostatic charge-discharge test was performed using automatic charge–discharge equipment (HJR-110mSM6, Hokuto Denko Co.) in a potential range of 3.0–4.2 V for 50 cycles. In the case of preparing a charged state electrode, the cell was fully charged by constant current charge with consecutive constant voltage charge for 5 h.

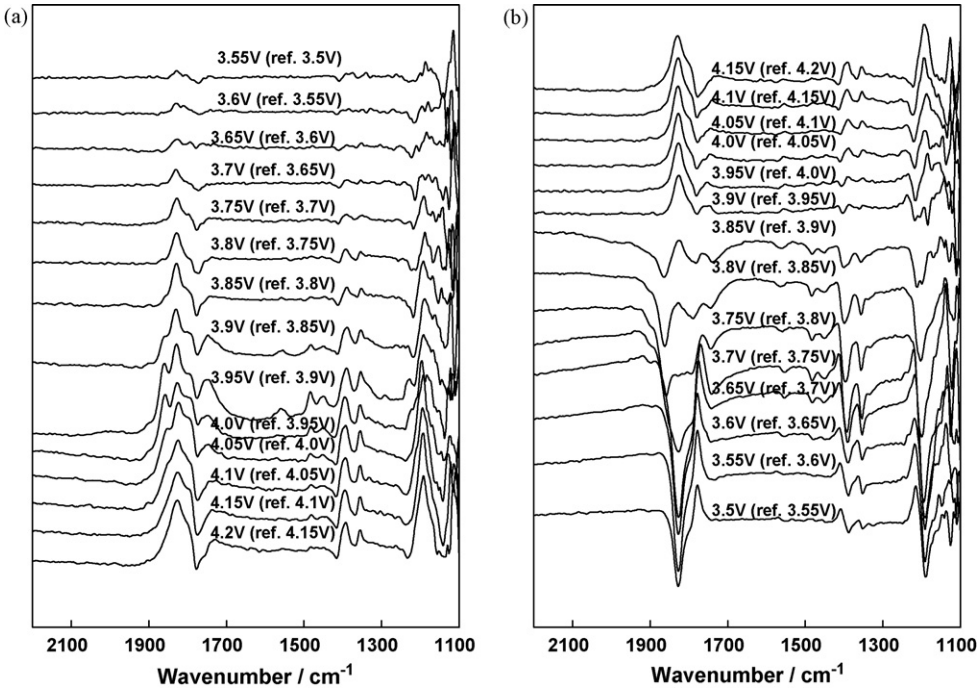

Fig. 5. *In situ* PM-FTIR spectra during cyclic voltammetry of $LiCoO_2$ thin film electrode in PC containing 1 mol dm^{-3} $LiClO_4$, (a) anodic polarization and (b) cathodic polarization.

This charged electrode was fully discharged by constant current discharge to prepare discharged one. The electrode surface was rinsed with pure DEC solvent to remove the Li-salt from the electrode surface. After that, the electrode was dried under high vacuum for 5 h to eliminate DEC solvent. The sample was set on sample holder for XPS analysis and put into an introduction chamber of XPS equipment. In this movement, a tightly sealed glass bottle was utilized to avoid a contact of the sample to atmosphere. XPS analysis was performed by using ESCA-3400 (Shimadzu Co.) with Mg Kα X-ray source (emission current: 10 mA, and acceleration voltage: 10 kV). Depth profiles of C, O, Cl and Co elements were measured by using ion gun controller HSE-800 (Shimadzu Co.). The emission current was 5 mA, and the accelerating voltage was 0.1 kV.

Ex situ AFM was performed by using Nano-Scope III (Digital Instruments Co.). Tapping mode was selected for AFM measurement mode in order to avoid the destruction of structure of surface film composed by organic species (there is some fear that the contact mode AFM breaks the surface film). AFM measurement was carried out to observe the morphology of $LiCoO_2$ thin film electrode surface. AFM samples were prepared based on the similar procedure as XPS analysis described above. Tapping mode AFM was measured in globe bag filled with pure Ar.

All electrochemical experiments were performed under dry Ar atmosphere at room temperature (25 °C). A water content of the electrolyte was less than 20 ppm, which was checked by Karl–Fischer titration method.

3. Results and discussion

Raman spectrum for sputtered $LiCoO_2$ thin film electrode was shown in Fig. 3. Only two peaks assigned to E_g and A_{1g} mode of $LiCoO_2$ was observed in this spectrum and it showed existence of no impurities [21]. Fig. 4 shows XRD patterns of $LiCoO_2$ films prepared by sputtering method for 30 and 90 min, with a pattern for the standard $LiCoO_2$ powder sample. From comparison of the XRD pattern of powder $LiCoO_2$ with that of the thin film, it can be seen that the thin film electrodes prepared by sputtering has a preferred orientation ((1 0 1) planes parallel to the substrate) [22]. In addition, the peak intensity of (1 0 1) plane was significantly different for two $LiCoO_2$ thin films, although the intensity of (0 0 3) plane was similar each other. In this way, the crystal orientation of $LiCoO_2$ thin film is strongly affected by substrate at the beginning of sputtering process. In this study, the $LiCoO_2$ thin film prepared by rf-sputtering for 90 min was employed for following several experiments.

Fig. 5 shows *in situ* PM-FTIR spectra of PC containing 1 mol dm^{-3} $LiClO_4$ during anodic and cathodic polarization. Fig. 6(a) shows FTIR spectrum of the electrolyte measured in absorbance mode. For comparison, some selected *in situ* PM-FTIR spectra collected during anodic scan and cathodic scan are shown in Fig. 6(b) and (c), respectively. In the case of anodic polarization, downward peaks were observed at 1780 cm^{-1}, which corresponded to C=O symmetric stretching vibration in decomposition product of PC. At the same electrode potential, upward peaks were also observed at 1830 cm^{-1}, which corresponded to C=O stretching vibration in PC. As shown in

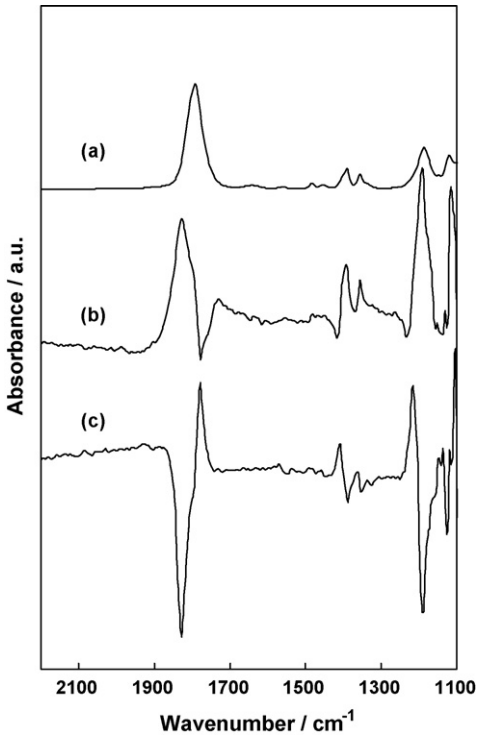

Fig. 6. (a) FTIR spectrum of PC containing 1 mol dm^{-3} $LiClO_4$, (b) *in situ* PM-FTIR spectrum during anodic polarization (4.2 V vs. Li/Li$^+$ ref. 4.15 V vs. Li/Li$^+$), and (c) *in situ* PM-FTIR spectrum during cathodic polarization (3.5 V vs. Li/Li$^+$ ref. 3.55 V vs. Li/Li$^+$).

Fig. 5(a), these peaks were observed at the electrode potential higher than 3.75 V vs. Li/Li$^+$. This phenomenon means that oxidation of PC occurs during charging process of $LiCoO_2$ and oxidation products of PC remain on $LiCoO_2$ electrode surface. Such a remaining product may form a kind of surface film. In addition, the electrode potential for the beginning of surface film formation well corresponded to the de-intercalation process of $LiCoO_2$, indicating that the oxidation process of PC could be strongly related to the redox potential of $LiCoO_2$. Detail of these

Table 1
Peak assignment for *in situ* FTIR spectra for the electrochemical oxidation of propylene carbonate containing 1.0 mol dm^{-3} $LiClO_4$ on the $LiCoO_2$ thin film

cm^{-1}	Upward peaks
1830	C=O stretching vibration in PC
1565	O–C=O bending vibration in PC
1485	CH_2 wagging vibration in PC
1455	CH_3 asymmetric bending in PC
1395	O–CH_2 wagging vibration in PC
1355	CH_3 symmetric bending vibration in PC
1190	C–O–C asymmetric stretching vibration in PC
	Downward peaks
1780	C=O symmetric stretching vibration in decomposition products
1420	CH_2 bending or CO_2 symmetric stretching vibration in decomposition products
1375	CH_3 symmetric bending vibration in decomposition products
1235	C–O–C asymmetric stretching vibration in decomposition products

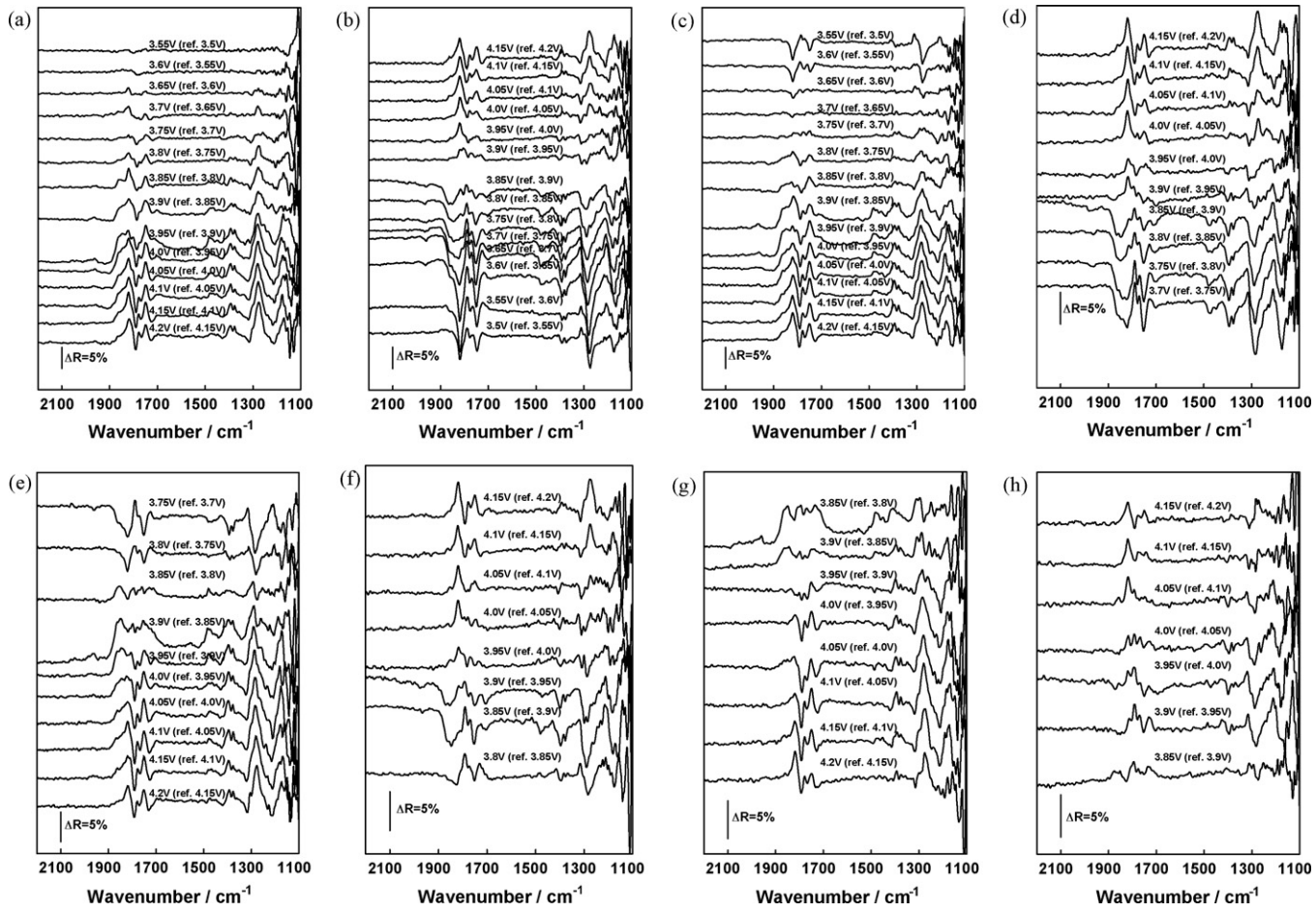

Fig. 7. *In situ* PM-FTIR spectra during cyclic voltammetry of $LiCoO_2$ thin film electrode in EC and DEC mixed solvent containing 1 mol dm^{-3} $LiClO_4$, (a) the first anodic polarization from 3.5 to 4.2 V vs. Li/Li^+, (b) the first cathodic polarization from 4.2 to 3.5 V vs. Li/Li^+, (c) the second anodic polarization from 3.5 to 4.2 V vs. Li/Li^+, (d) the second cathodic polarization from 4.2 to 3.7 V vs. Li/Li^+, (e) the third anodic polarization from 3.7 to 4.2 V vs. Li/Li^+, (f) the third cathodic polarization from 4.2 to 3.8 V vs. Li/Li^+, (g) the fourth anodic polarization from 3.8 to 4.2 V vs. Li/Li^+, and (h) the fourth cathodic polarization from 4.2 to 3.85 V vs. Li/Li^+.

peaks was similar to some reports of our group and already discussed in these papers [8–11]. The summary of assignment of peaks was listed in Table 1.

Fig. 5(b) shows *in situ* PM-FTIR spectra during cathodic polarization. At the beginning of cathodic polarization, the oxidation of PC was still observed. But, the shape of each spectrum gradually changed in the range of more cathodic electrode potential than 3.9 V vs. Li/Li^+. Finally, upward peaks at 1780 cm^{-1} and downward peaks at 1830 cm^{-1} were observed at 3.6 V vs. Li/Li^+. A similar spectrum change was observed for other peaks appeared at lower wavenumber. Most possible understanding of these spectra is given by stripping and dissolving of surface film during cathodic polarization. The same phenomenon was observed in the case of EC-DEC binary solvent system.

Fig. 7 shows *in situ* PM-FTIR spectra of EC-DEC binary solvent containing 1 mol dm^{-3} $LiClO_4$ during cyclic voltammetry. Fig. 8(a) shows FTIR spectrum of the electrolyte measured in absorbance mode. For comparison, some selected *in situ* PM-FTIR spectra collected during anodic scan and cathodic scan are shown in Fig. 8(b) and (c), respectively. Formation and stripping of surface film in the first cycle were confirmed. Observed peaks were almost the same as data reported in our paper and summary of peak assignment was shown in Table 2. Fig. 7(a) and (b) show *in situ* PM-FTIR spectra during the first anodic polarization and cathodic polarization, respectively. During the cathodic scan, the stripping process of surface film was observed

Table 2
Peak assignment for *in situ* FTIR spectra for the electrochemical oxidation of ethylene carbonate and diethyl carbonate containing 1.0 mol dm^{-3} $LiClO_4$ on the $LiCoO_2$ thin film

cm^{-1}	Upward peaks
1820	C═O stretching vibration in EC
1750	C═O stretching vibration in DEC
1395	CH_2 wagging vibration in EC
1375	CH_3 symmetric bending in DEC
1275	C–O–C asymmetric stretching vibration in DEC
1170	C–O–C asymmetric stretching vibration in EC
	Downward peaks
1790	C═O symmetric stretching vibration in decomposition products
1730	C═O symmetric stretching vibration in decomposition products
1425	CH_2 bending vibration in decomposition products
1320	C–O–C asymmetric stretching vibration in decomposition products
1205	C–O–C symmetric stretching vibration in decomposition products

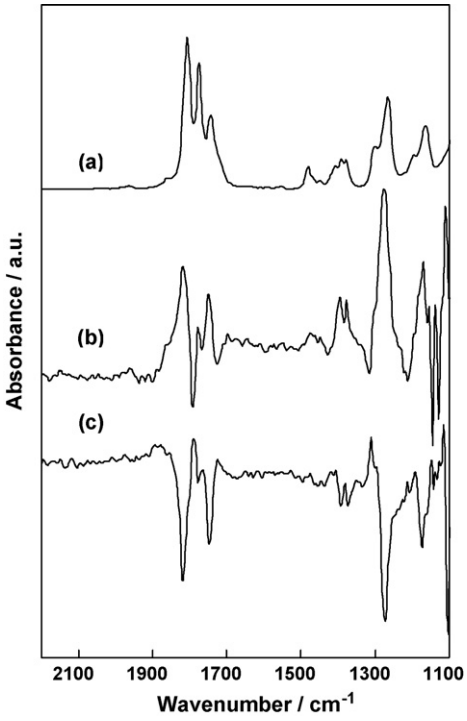

Fig. 8. (a) FTIR spectrum of EC-DEC contaning 1 mol dm^{-3} $LiClO_4$, (b) *in situ* PM-FTIR spectrum during anodic polarization (4.2 V vs. Li/Li^+ ref. 4.15 V vs. Li/Li^+), and (c) *in situ* PM-FTIR spectrum during cathodic polarization (3.5 V vs. Li/Li^+ ref. 3.55 V vs. Li/Li^+).

at the electrode potential lower than 3.9 V vs. Li/Li^+. In order to discuss the instability of surface film on $LiCoO_2$, *in situ* PM-FTIR spectroscopy was performed during several cycles of cyclic voltammetry. Fig. 7(c) and (d) show the *in situ* PM-FTIR spectra during the second cycle. All peaks appeared at almost the same wavenumber, compared with the first cycle. The second cathodic polarization was stopped at the potential of 3.7 V vs. Li/Li^+. At this potential, the surface film stripping process was still continuing, so that the third anodic polarization was started before finishing surface film stripping process. With shifting of the lower limit potential toward more anodic direction for cyclic voltammetry, the peak intensities for surface film formed during the third anodic polarization were decreased. In the following steps, similar phenomenon was observed. The third cathodic polarization was stopped at 3.8 V vs. Li/Li^+, and the fourth anodic polarization started from 3.8 V vs. Li/Li^+, then the peak intensities for the surface film formation further decreased. In this way, remaining surface film on $LiCoO_2$ depends on electrode potential. When adequate amount of surface film adsorbs on $LiCoO_2$ surface, oxidation of electrolyte can be suppressed. It is obvious that the surface film formation and stripping process on $LiCoO_2$ does not occur only in the first cycle, but also in the second and later cycles. This phenomenon is due to a weak adsorption of oxidation products from electrolyte, such as electrostatic interaction between dipole moment of products and electrode surface. Such kind of interaction might be related to surface potential of electrode, which is changed by electrode potential. In the following discussion, we have confirmed this phenomenon by using other analytical techniques.

Fig. 9 shows XPS spectra of C 1s for charged and discharged $LiCoO_2$ thin film electrode. In both spectra, one sharp peak was observed at 284.5 eV corresponding to hydrocarbon and another broad peak was observed around 288.8 eV corresponding to carbonate groups involved in polymerized carbonates produced by decomposition of electrolyte. The C 1s peak from poly-oxyethylene group was also observed at 285.5 eV as a small shoulder.

Fig. 10 shows XPS spectra of O 1s, Cl 2p and Co 2p for these electrodes. In the XPS spectra of O 1s shown in Fig. 8(a) and (b), two peaks were observed. One of these peaks was observed at 529–529.5 eV corresponding to oxygen of $LiCoO_2$ and the other was observed at 531.5 eV corresponding to lithium carbonate and some poly-oxyethylene groups. The origin of this

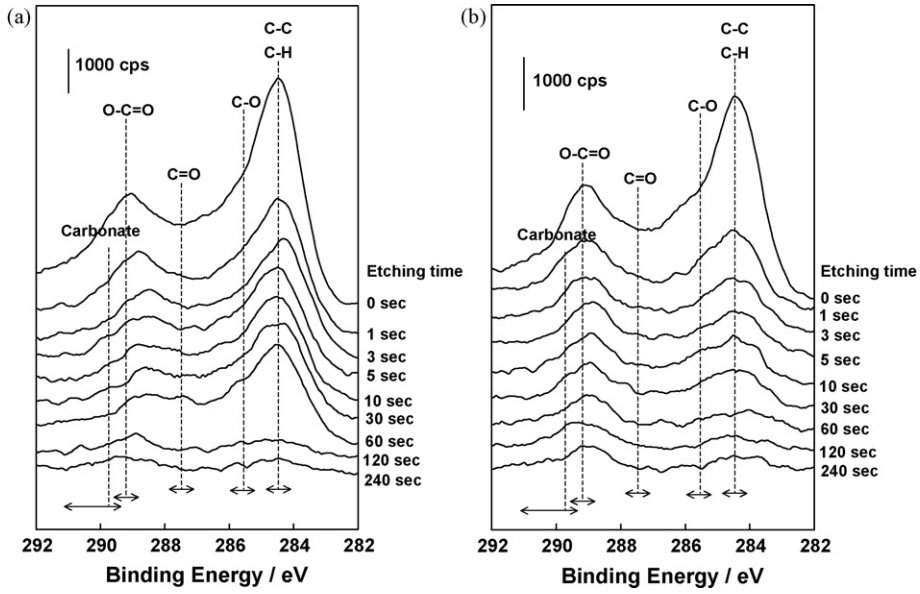

Fig. 9. XPS spectra of C 1s for $LiCoO_2$ thin film electrodes, (a) charged to 4.2 V vs. Li/Li^+ and (b) discharged to 3.0 V vs. Li/Li^+.

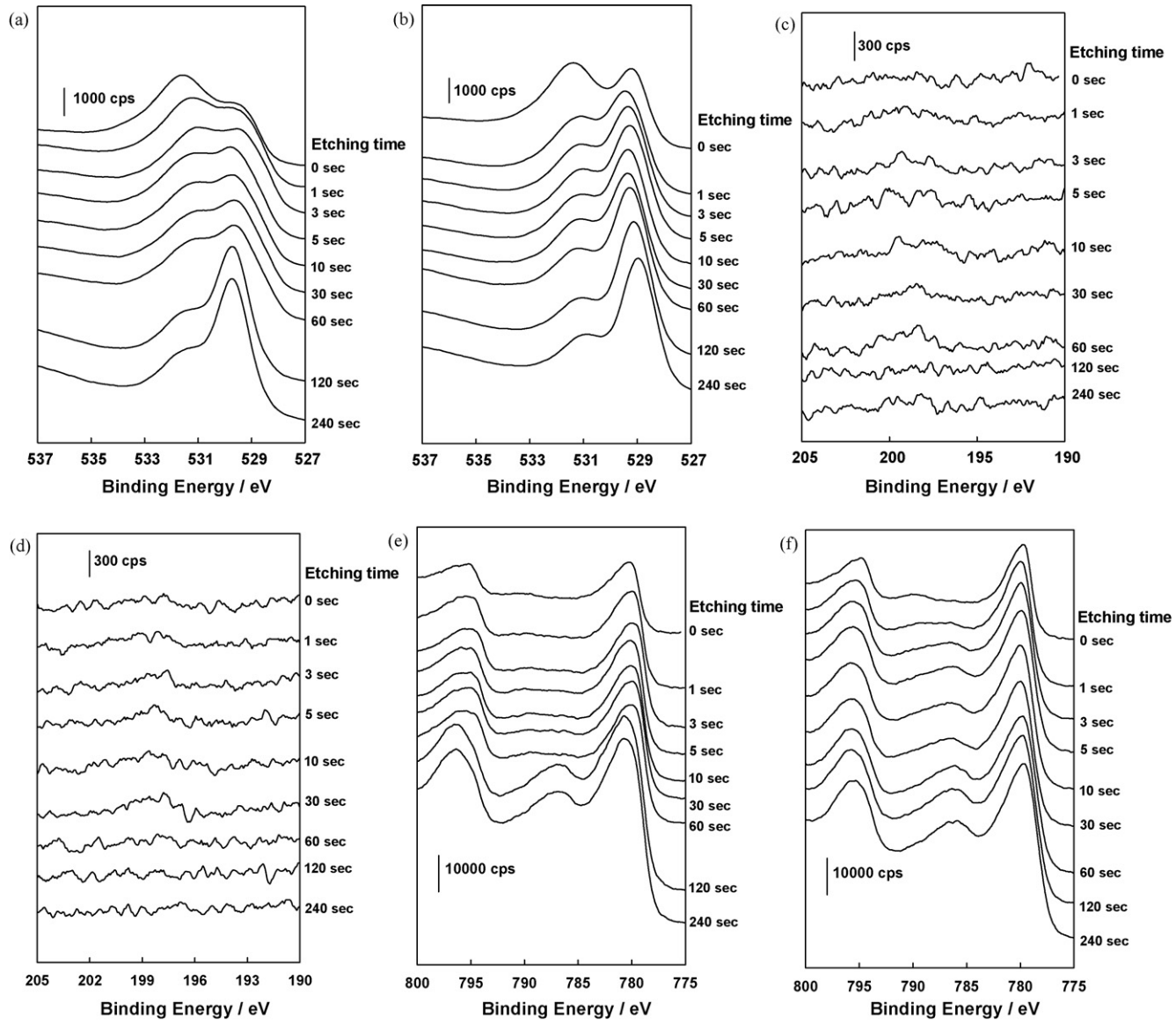

Fig. 10. XPS spectra of O 1s, Cl 2p and Co 2p for $LiCoO_2$ thin film electrodes, (a) O 1s for charged electrode, (b) O 1s for discharged electrode, (c) Cl 2p for charged electrode, (d) Cl 2p for discharged electrode, (e) Co 2p for charged electrode, and (f) Co 2p for discharged electrode.

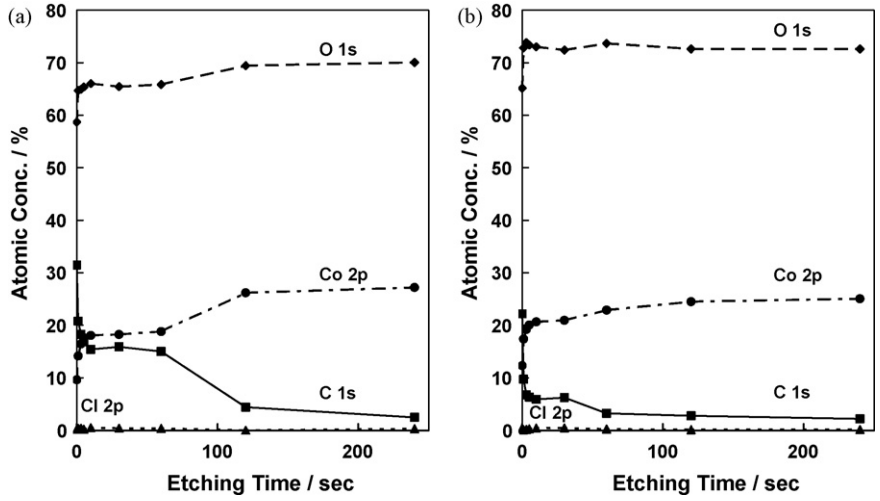

Fig. 11. Depth profiles of C, O, Cl and Co elements involved in $LiCoO_2$ thin films. (a) Charged to 4.2 V vs. Li/Li^+ and (b) discharged to 3.0 V vs. Li/Li^+.

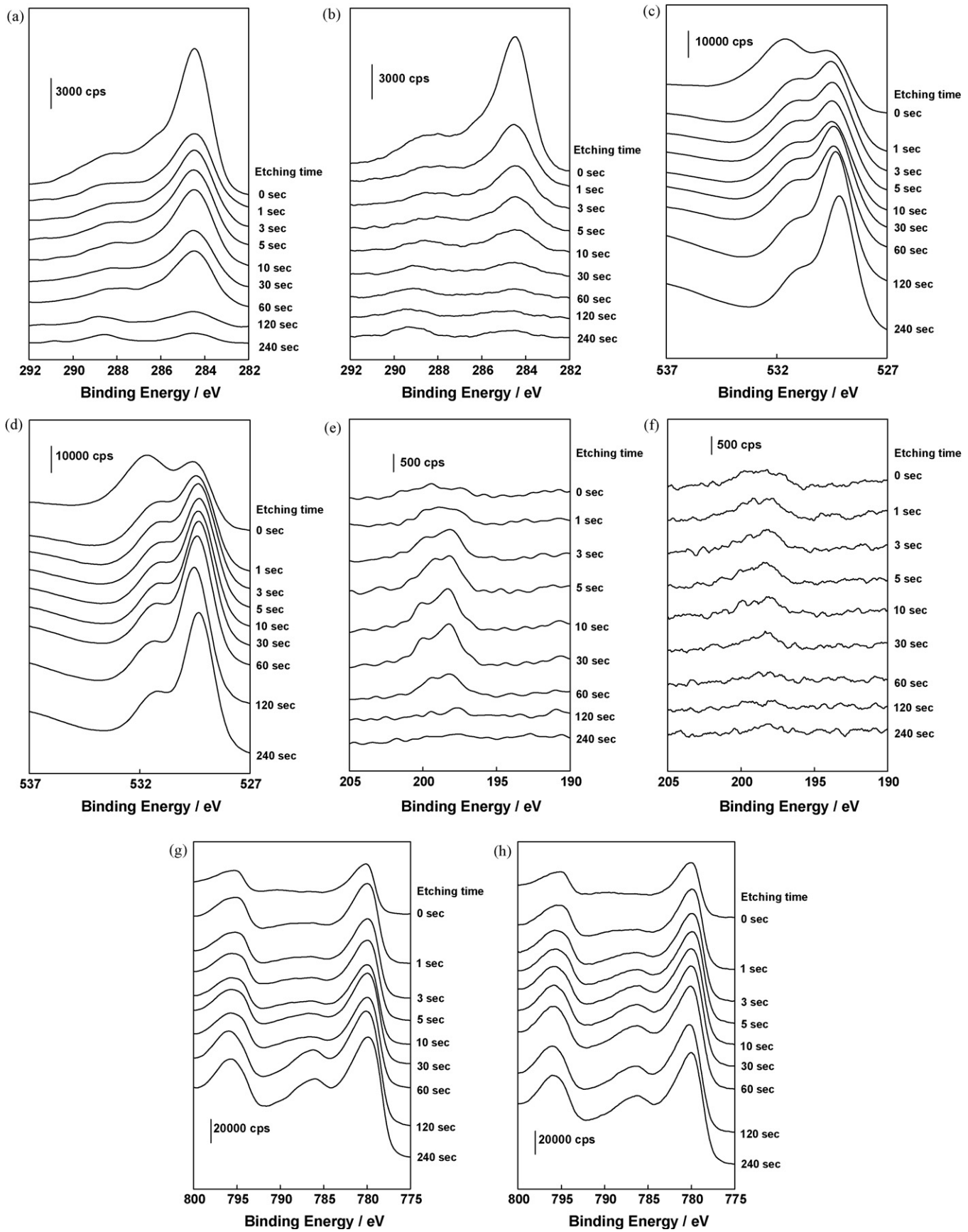

Fig. 12. XPS spectra of C 1s, O 1s, Cl 2p and Co 2p for $LiCoO_2$ thin films after 50 cycles of charge–discharge, (a) C 1s for charged electrode, (b) C 1s for discharged electrode, (c) O 1s for charged electrode, (d) O 1s for discharged electrode, (e) Cl 2p for charged electrode, (f) Cl 2p for discharged electrode, (g) Co 2p for charged electrode, and (h) Co 2p for discharged electrode.

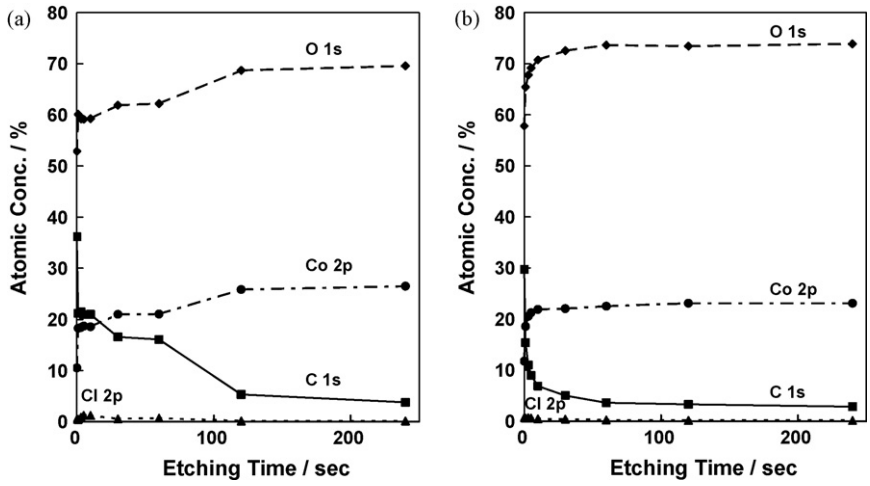

Fig. 13. Depth profiles of C, O, Cl and Co elements involved in $LiCoO_2$ thin films after 50 cycles of charge–discharge, (a) charged to 4.2 V vs. Li/Li^+ and (b) discharged to 3.0 V vs. Li/Li^+.

poly-oxyethylene groups are supposed to be the decomposition of EC and DEC. From these results, it can be said that these solvents are oxidized to form polymer like compounds remaining on $LiCoO_2$ surface as surface film. Fig. 10(c) and (d) shows XPS spectra of Cl 2p. Both spectra had no clear peak, showing that the surface film did not contain chlorinated species originated from ClO_4^- anion. In this way, the surface film was mainly consisted of organic species originated from EC and DEC [7].

Elemental depth profiles for these electrodes were shown in Fig. 11. Surface film of charged electrode was thicker than that of discharged one, indicating that the surface film was stripped

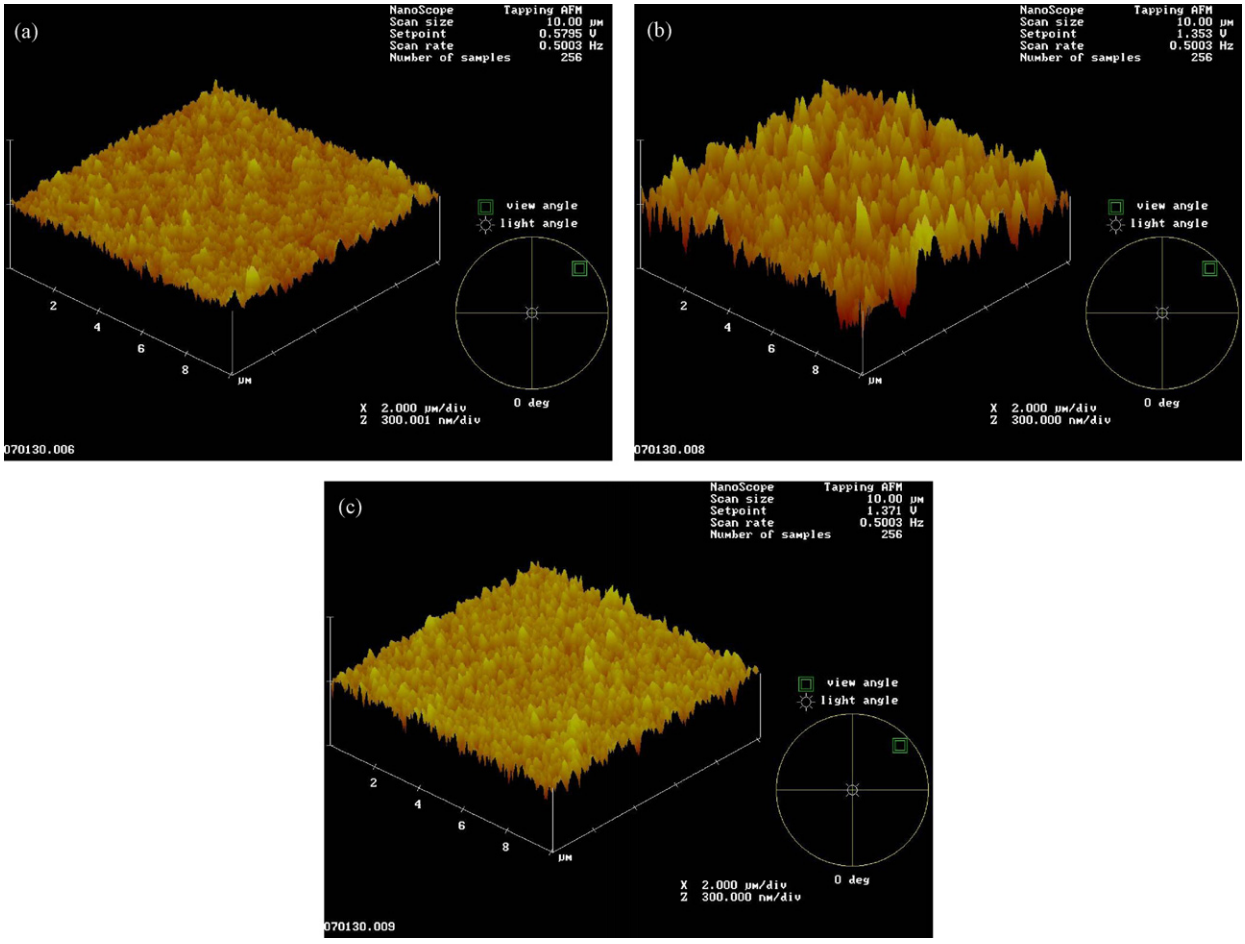

Fig. 14. Tapping mode AFM image for $LiCoO_2$ thin films, (a) as-prepared, (b) charged to 4.2 V vs. Li/Li^+, and (c) discharged to 3.0 V vs. Li/Li^+.

off during discharge process. This result agrees with the result of *in situ* PM-FTIR measurement.

Fig. 12 shows the XPS spectra of C 1s, O 1s, Cl 2p and Co 2p for $LiCoO_2$ thin film electrode after discharge and charge cycles. The elemental depth profiles were shown in Fig. 13. In the case of Cl 2p, small peak corresponding to LiCl was observed at 198 eV. From this spectrum, it can be said that solvent does not only decompose during charge–discharge process, but also ClO_4^- anion decomposes. However, the amount of Cl was much smaller than those of other elements. These spectra and depth profile were almost the same with the spectra for $LiCoO_2$ electrode after the first cycle. From these spectra, it is proposed that the formation and stripping process of surface film is repeated in every cycle on $LiCoO_2$ thin film electrode surface.

AFM images of $LiCoO_2$ thin film electrode after charge and discharge process are shown in Fig. 14. An image of as-prepared $LiCoO_2$ thin film electrode is shown in Fig. 14(a). In comparison of the image for charged electrode (Fig. 14(b) with that for the discharged electrode Fig. 14(c)), it can be clearly seen that the former surface is rougher, compared to the latter one. And the discharged one had almost the same roughness with that of as-prepared one (Fig. 14(a)). This surface morphology change indicates that electrochemically decomposed products deposit on the electrode surface and finally cover whole electrode surface during charge process. However, during discharge process, decomposed products strip off from the electrode surface and then a fresh surface appears again. These images also agree with observation from *in situ* PM-FTIR and XPS.

4. Conclusion

Formation and stripping process of the surface films on the $LiCoO_2$ thin film electrodes prepared on gold substrate was investigated by using *in situ* PM-FTIR, XPS, and AFM. *In situ* PM-FTIR analysis showed that the solvent of electrolyte solution, such as PC or EC-DEC binary solvent, was oxidized to form surface film at the electrode potential of 3.75 V vs. Li/Li^+ and higher, during charge process. However, the surface film is not so stable and strips off during discharge process, due to weak interaction between the surface film and $LiCoO_2$ thin film electrode surface.

C 1s XPS spectra for charged and discharged $LiCoO_2$ thin film electrode showed that oxidized product from electrolyte solution formed polymerized carbonate species as surface film. Depth profile of XPS spectra for charged and discharged electrodes proved that charged one had thicker surface film than discharged one.

AFM observation showed the difference in surface morphology between charged and discharged $LiCoO_2$ thin film electrodes. Charged electrode had rougher surface compared to discharged one.

From the results of three analytical techniques, it can be concluded that the surface film on $LiCoO_2$ is not stable and shows dynamic behavior during charge–discharge process. This dynamic behavior could be strongly related to the stability of positive electrode during long discharge and charge cycles.

References

[1] J.-M. Tarascon, M. Armand, Nature 414 (2001) 359–367.
[2] T. Nagaura, K. Tozawa, Prog. Batt. Sol. Cells 9 (1990) 209.
[3] D. Aurbach, B. Markovsky, M.D. Levi, E. Levi, A. Schechter, M. Moshkovich, Y. Cohen, J. Power Sources 81–82 (1999) 95–111.
[4] S.A. Cambell, C. Bowes, R.S. McMillan, J. Electroanal. Chem. 284 (1990) 195.
[5] F. Ossola, G. Pistoria, R. Seeber, P. Ugo, Electrochim. Acta 33 (1988) 47.
[6] Y. Matsuo, R. Kostecki, F. McLrnon, J. Electrochem. Soc. 148 (2001) A687–A692.
[7] K. Edstrom, T. Gustafsson, J.O. Thomas, Electrochim. Acta 50 (2004) 397–403.
[8] K. Kanamura, T. Umegaki, M. Ohashi, S. Toriyama, S. Shiraishi, Z. Takehara, Electrochim. Acta 47 (2001) 433–439.
[9] K. Dokko, T. Matsushita, K. Kanamura, Electrochemistry (Tokyo, Jpn.) 73 (2005) 54–59.
[10] T. Matsushita, K. Dokko, K. Kanamura, J. Power Sources 146 (2005) 360–364.
[11] T. Matsushita, K. Dokko, K. Kanamura, J. Electrochem. Soc. 152 (2005) A2229–A2237.
[12] R. Fong, U. Von Saken, J.R. Dahn, J. Electrochem. Soc. 137 (1990) 2009–2013.
[13] Y. Matsumura, S. Wang, J. Mondori, J. Electrochem. Soc. 142 (1995) 2914–2918.
[14] S.-K. Jeong, M. Inaba, Y. Iriyama, T. Abe, Z. Ogumi, J. Power Sources 119–121 (2003) 555–560.
[15] H. Ota, Y. Sakata, A. Inoue, S. Yamaguchi, J. Electrochem. Soc. 151 (2004) A1659–A1669.
[16] X. Zhang, R. Kostecki, T.J. Richardson, J.K. Pugh, P.N. Ross Jr., J. Electrochem. Soc. 148 (2001) A1341–A1345.
[17] J. Ying, C. Wan, C. Jiang, J. Power Sources 102 (2001) 162–166.
[18] S.M. Lee, S.H. Oh, W.I. Cho, H. Jang, Electrochim. Acta 52 (2006) 1507–1513.
[19] B. Beden, C. Lamy, Spectroelectrochemistry, Plenum Press, New York, 1988, pp. 223–259.
[20] W.N. Richmond, P.W. Faguy, R.S. Jackson, S.C. Weibel, Anal. Chem. 68 (1996) 621–628.
[21] M. Inaba, Y. Iriyama, Z. Ogumi, Y. Todzuka, A. Tasaka, J. Raman Spectrosc. 28 (1997) 613–617.
[22] J.B. Bates, N.J. Dudney, B.J. Nedecker, F.X. Hart, H.P. Jun, S.A. Hackney, J. Electrochem. Soc. 147 (2000) 59–70.